Civil Engineering Infrastructures Journal xx,xx
DOI: 10.22059/ceij.2024.371955.2012

Probabilistic Analysis of Braced Excavation for Box Drain Construction in Cuttack

Author name: Pratima Kumari[1], Avijit Burman [2], Pijush Samui[3*]

[1]Post Graduate Student, Department of Civil Engineering, National Institute of Technology, Patna, India, pratimak.pg21.ce@nitp.ac.in

[2]Associate Professor, Department of Civil Engineering, National Institute of Technology, Patna, India, avijit@nitp.ac.in

[3] Professor, Department of Civil Engineering, National Institute of Technology, Patna, India, pijush@nitp.ac.in

(* Corresponding Author)

Received: 08/02/2024
Revised: 09/07/2024
Accepted: 05/08/2024

Abstract

This study presents a probabilistic failure analysis of a braced excavation system for a 9.0 m deep box drain in Cuttack, Odisha, using Monte Carlo Simulation (MCS) and Subset Simulation (SS) methods. The drain spans 3.0 km through highly plastic clayey soil with low shear strength, requiring excavation and braced techniques. Geotechnical field exploration suggests that the soil along the 3.0 km long stretch of the proposed box drain site has very wide variation. A probabilistic analysis is conducted to ascertain the risk involved in the designed braced excavation system. In probabilistic analysis of the braced excavation system, cohesion and unit weight of soil are treated as lognormal distributed random variables. Spatially correlated random fields along the depth are generated using Pearson Correlation matrix and Markov Correlation function. MCS with 10000 samples have been run to conduct the probabilistic response of the braced excavation system. The paper also presents the results of SS, an advanced version of MCS that enables rapid probabilistic analysis. Furthermore, the results obtained using MCS and SS are compared to establish the relative superiority of SS over MCS.

Keywords: Braced cut, Probabilistic Analysis, Random Field, Cross-Correlation, Monte Carlo Simulation, Subset Simulation

1. Introduction

Underground infrastructure construction is increasingly being considered in densely populated urban areas to optimise land utilisation. Braced excavation systems (BES) are often used in places with deep deposits of soft clay, and excavation is required to reach the desired foundation level or for some other purpose (Farzi et al. 2018). Braced excavation is a method where deep excavations with straight vertical faces are laterally supported by a sheeting and bracing system until the structure is built. The design of braced cuts involves two distinct but interrelated features, namely, stability of excavation, ground movement, control of water into the excavation, effect of adjoining structures and so on. In deep excavations creating a safe slope on the excavation face is generally not feasible due to high cost, unavailability of space etc. So, the excavation is temporary supported by sheets/walls and struts, which are removed individually when their requirements cease.

One crucial aspect of BES design is to ensure the structural integrity and safety of the bracing system. To calculate the stresses exerted on the struts in braced excavations, empirical methods like as the Apparent Pressure Diagram (APD) are widely used. Various researchers (Peck 1969; Terzaghi et al. 1996; Zhang et al. 2021; Dan and Sahu 2022; Han et al. 2023) advocated the use of the APD to assess the amount and distribution of prop loads in braced excavations for different soil types, such as sands, strong fissured clays, and soft to medium clays. The uncertainties associated with variation of soil properties along the depth can negatively affect the stability and safety of the BES. Therefore, it is of utmost importance to consider these uncertainties during design and analysis of the BES. Several researchers (Sekhavatian and Janalizadeh Choobbasti 2018a; He et al. 2020; Zhang and Liu 2022; Zhao et al. 2022; Zhang et al. 2024) have used different approaches for probabilistic analysis (PA) for braced cut. (Luo et al. 2012) used an equivalent variance technique to consider the spatial variability so that PA using First order random field technique of basal heave braced excavation failure can be accessed. It was noticed that First Order Reliability Method (FORM)(Zhang et al. 2019) and Monte Carlo Simulation (MCS) technique produce almost similar results. (Luo and Das 2016) used the system-level probabilistic serviceability assessment approach for braced excavations in clays. The authors used MCS to generate multiple realizations of the random variables, and evaluated the system-level reliability index (β). (Qi and Zhou 2017) investigated braced excavation in a three-step procedure. First, a braced excavation's finite element model was created, taking bracing systems into account as well as impacts of the interaction between the soil and the structure. Also, a PA was conducted in order to account for the uncertainties associated with back analysis. (Chowdhury 2017) presented a reliability analysis (RA) of excavation-induced basal heave, concentrating on determining the stability of deep excavations while taking ground movements at the excavation's base into consideration to assess the excavation system's vulnerability. (Sekhavatian and Janalizadeh Choobbasti 2018b) presented a deep excavation RA utilising the response surface and MCS methodologies. (Luo et al. 2018) performed finite element modelling to predict the excavation-induced wall and ground movement and concluded that system probability of serviceability failure is greater than or equal to that for each single failure mode.

It is a known fact that soil parameters are correlated to each other, and it is necessary to determine the relative contributions of these factors on the overall stability of the system. (Cho and Park 2010) highlighted the importance of considering spatial variability cross-correlation for analysing and designing strip footings. The choice of cross-correlation coefficient between the soil parameters are important factor for correct estimation of probability of failure (P_f) of any geotechnical structure. (Javankhoshdel and Bathurst 2016a) investigated the influence of cross-correlation between soil parameters on the P_f for simple cohesive and c-ϕ soil slopes. (Nguyen

and Chowdhury 1985) identified the possible correlation between random values of the shear strength parameter that can impact the likelihood of failure for slopes. Recently, (Ahmad et al. 2024) conducted a probabilistic analysis particularly in railway embankment using subset simulation by incorporating machine learning techniques. (Sabri et al. 2024) performed the SS and MCS technique using excel spreadsheet environment to estimate the reliability of a soil slope.

In the current study, the effect of cross-correlation of cohesive soil parameters on P_f of a braced excavation has been examined. MCS and SS techniques have been utilized to estimate the P_f of a BES for construction of a box drain in the city of Cuttack, India. SS is an advanced version of MCS developed by more (Au and Wang 2014) that requires relatively smaller number of samples compared to MCS for predicting P_f with desired accuracy. The risk analyses have been carried out for developing random realizations of the soil parameters (i.e., cohesion and unit weight) along the depth of the braced cut. The effects of correlation between the soil parameters on the probability of failure is also investigated. The study is helpful for estimating the risk of failure for the safety of the construction.

2. Research Significance

The probabilistic failure response of large and important civil engineering project should ideally be carried out to determine the confidence level in the designed system. FORM, second order reliability method, first order second moment method, MCS and SS are some of the techniques which have been used successfully in the past by the investigators (Wong 1985; Lee and Kwak 1987; Juang et al. 2019; Yang and Ching 2019; Low 2021). However, the study of the past literatures show that Subset simulation method has rarely been used for PA of BES. To obtain reliable results using MCS, it is necessary to consider a large number of samples i.e., in the order of 10000 or more (Au and Wang 2014). SS is an advanced version of MCS in which the PA is carried out in few levels. The samples in each level are generated in a way such that they are shifted towards failure region in subsequent levels, and thus the failure response of the system can be quickly simulated in SS analysis utilizing less samples compared to MCS. In the present paper, the results of PA of a BES using SS of a real-life project is reported. A 9.0 m deep cut is supported with braced excavation technique for construction of box drain in the state of Cuttack, Orissa, India. The results have been further compared with the results obtained using MCS to establish the relative superiority of SS over MCS. The spatially variable and cross-correlated random fields of cohesion and unit weight are developed for representing the uncertainties arising due changes in soil properties within the domain. The failure probabilities of the system are presented for both correlated as well as uncorrelated. The authors believe that the present work can shed important light over the probabilistic failure response of deep excavation projects.

3. Study area

The study area is the City of Cuttack in the state of Orissa situated at latitude 20^0 31’23” & 20^0 52’30” North and longitude 85^0 47’17” & 85^0 78’80” East. The state government has undertaken a project to construct a box drain for a 3.0 km long stretch inside the city. The construction of box drain requires excavation up-to 8.0 – 9.0 m depth from the present ground level. Fig. 1(a) presents the 3.0 km long alignment of the box drain to be constructed in the city of Cuttack. Fig. 1(b) shows the details of the box drain. It should be noted that the soil below the box drain has very low shear strength necessitating the low shear strength soil below the box drain level should be replaced by coarse sand of 3.0 m depth. Therefore, it is necessary to excavate up to 9.0 m depth from the ground level.

Extensive site investigation was carried out to determine the necessary geotechnical parameters of the soil in the construction site. Soil samples were collected from a total of 31 boreholes dug at the site along the 3.0 km long stretch each extending at distance of 100.0 m of the proposed box drain. All necessary geotechnical parameters such as grain size distribution, Atterberg limits, cohesion, unit weight, moisture content, compression index was determined in the laboratory. However, only cohesion and the unit weight values along the depth of different boreholes have been gathered at various chainage locations as shown in Fig. 2(a) and Fig. 2(b) because these two parameters are primarily required for braced excavation analysis. Note that in this current study, analysis results have been done at chainage distance 3+310 only.

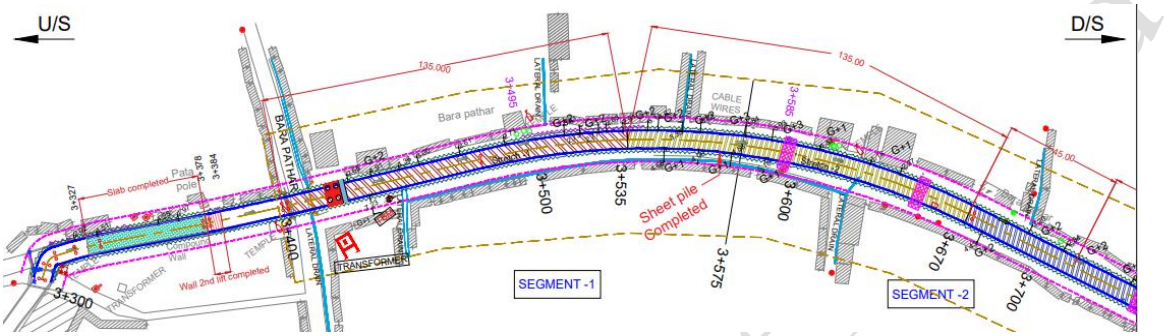

Fig. 1(a) 3.0 km long alignment of the box drain in Cuttack, Odisha

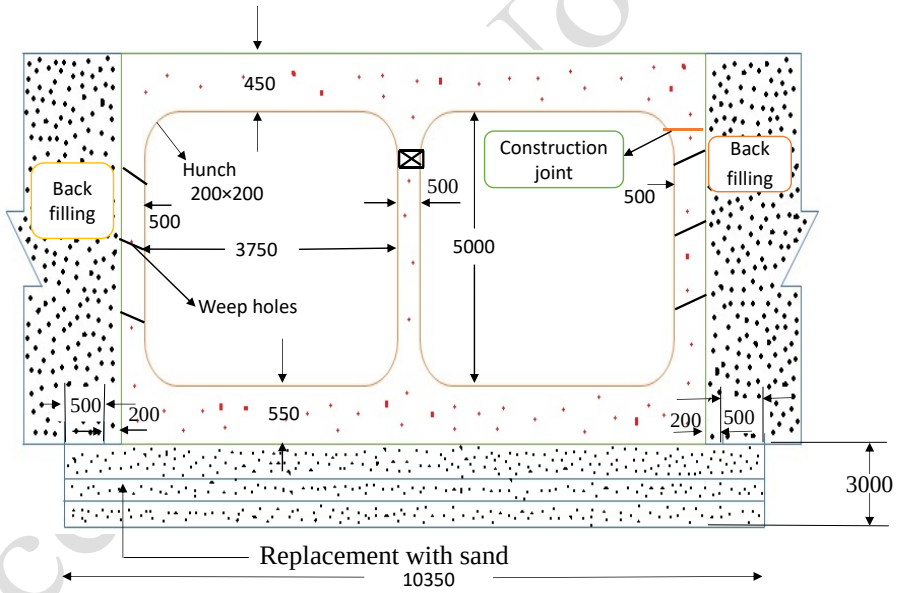

Fig. 1(b) Proposed Box Drain Profile (All dimension is in mm)

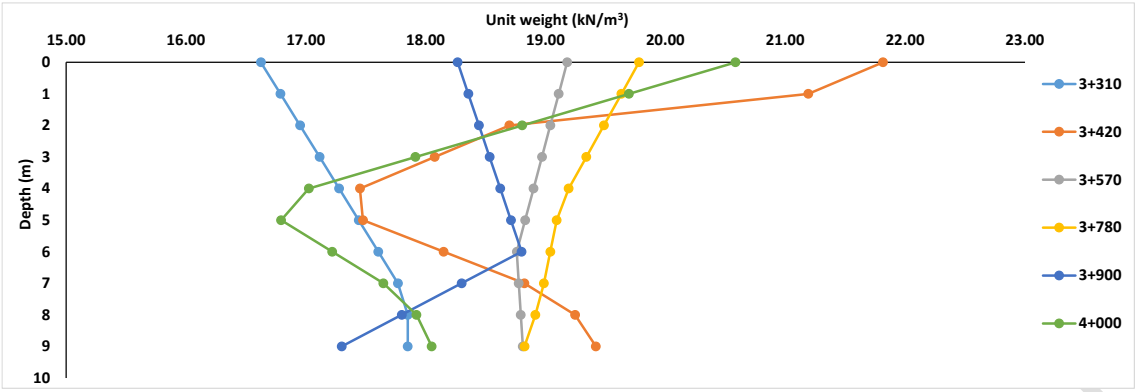

Fig. 2(a) Mean value of unit weight along the depth for a bore hole at various chainage distances

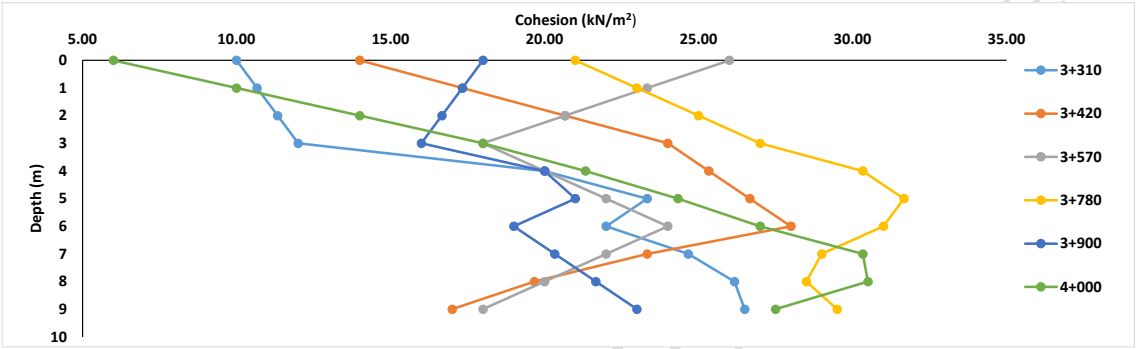

Fig. 2(b) Mean value of cohesion along the depth for a bore hole at various chainage distances

4. Methodology

The Lateral earth pressure (LEP) in a braced cut depends on soil type, construction method, and equipment. The LEP varies because of spatial changes in soil parameters both horizontally and vertically. For the braced cuts viz., (1) design of cuts in sand (2) design of cuts in clay, researchers (Peck 1969; Sivakugan and Das 2009) proposed an APD as shown in Fig. 3. The APD of cuts in sand, soft and medium clay, and stiff clay are depicted in Fig. 3(a), Fig. 3(b) and Fig. 3(c) respectively. The magnitude of lateral APD (σ_a) is shown in Eq. 1. (Peck 1969) classified clays based on the non-dimensional stability number (N_s) as expressed in Eq. 3. The value of $N_s > 4$ indicates the soft to medium clay and $N_s < 4$ stands for stiff clay. Eqs. 4 and 5 present the value of σ_a for the soft to medium clay and stiff clay, respectively.

$$\sigma_a = 0.65\gamma H K_a \tag{1}$$

$$K_a = \tan^2\left(45° - \frac{\phi'}{2}\right) \tag{2}$$

$$N_s = \frac{\gamma H}{c} \tag{3}$$

$$\sigma_a = \gamma H\left[1 - \left(\frac{4c}{\gamma H}\right)\right] \text{ and } \sigma_a = 0.3\gamma H \text{ (whichever is more)} \tag{4}$$

$$\sigma_a = 0.2\gamma H \text{ to } 0.4\gamma H \quad \text{(With an average of } 0.3\gamma H\text{)} \tag{5}$$

where, c = undrained cohesion, $\phi' =$ effective angle of internal friction, γ = unit weight of soil, K_a= Rankine active pressure coefficient.

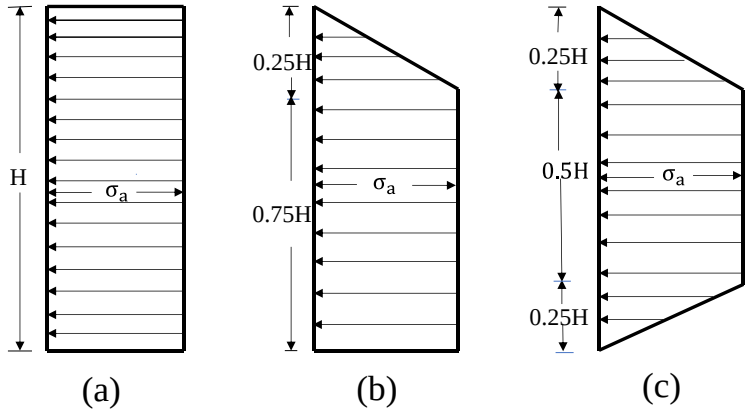

Fig. 3 APD envelope of (a) Sand, (b) Soft to medium clay and (c) Stiff clay Source:(Peck 1969)

The soil sample in the study area is mostly cohesive soil. It has been observed that the soil parameters (i.e., c' and γ) vary depending on the excavation depth. Since different clay layers have been encountered in the cut, the average value of c' and γ can be calculated using Eq. 6 and Eq. 7 as follows:

$$c_{av} = \frac{1}{H}(c_1H_1 + c_2H_2 + \cdots + c_nH_n\ ) \tag{6}$$

$$\gamma_{av} = \frac{1}{H}(\gamma_1H_1 + \gamma_2H_2 + \cdots + \gamma_nH_n\ ) \tag{7}$$

4.1. Load on strut

Bracing strut and excavation bracing frame supports braced excavation by propping the vertical face (Bahrami 2019). This research employs four designated struts (A, B, C, D) shown in Fig. 4. Additionally, sheet piles are assumed to have hinges at struts B and C. Including hinges at struts B and C increases shear forces and bending moments, ensuring a conservative design. The forces $F_A, F_B, F_C,$ and F_D are the reaction forces (per unit length) at the strut levels. The reaction forces were determined through equilibrium calculations. The load on the strut can be accomplished by utilizing the formula $P_i = F_i s_i$ (i = A, B, C and D). Notably, subscripts P, F, and s denote the load, force, and spacing between strut levels, respectively, while superscript i indicates the strut level. Interested readers can refer to the works of (Sivakugan and Das 2009) for further details on braced excavation procedures.

4.1.1. Sheet piles

A steel sheet pile has been used to support the braced cut. Calculations are performed to determine the maximum bending moment (M_{max}) for each of the sections depicted in Fig. 4(b). The section modulus (S) of the sheet pile can be calculated using Eq. 8.

$$S = \frac{M_{max}}{\sigma_{all}} \tag{8}$$

Here, σ_{all}= allowable flexural yield stress of steel.

4.1.2. Wales

Steel structural members that transfer load from the diaphragm wall to the strut are called Wales. Wales is fastened to the sheet pile at points meeting lateral support requirements. Fig. 4(a) depicts the basic installation structure of braced cut. The maximum moment for the pinned connection of the Wales at any level can be determined using Eq. 9. The factor of safety (FOS) is defined using Eq. 10 based on the maximum 'S' value available at the site. This study reports the maximum value of S = 2000 cm^3 at the site.

$$M_{max} = \frac{F_i(s_i)^2}{8} \tag{9}$$

$$FOS = \frac{\text{maximum section modulus of Wales}}{\text{available section modulus}} \quad (10)$$

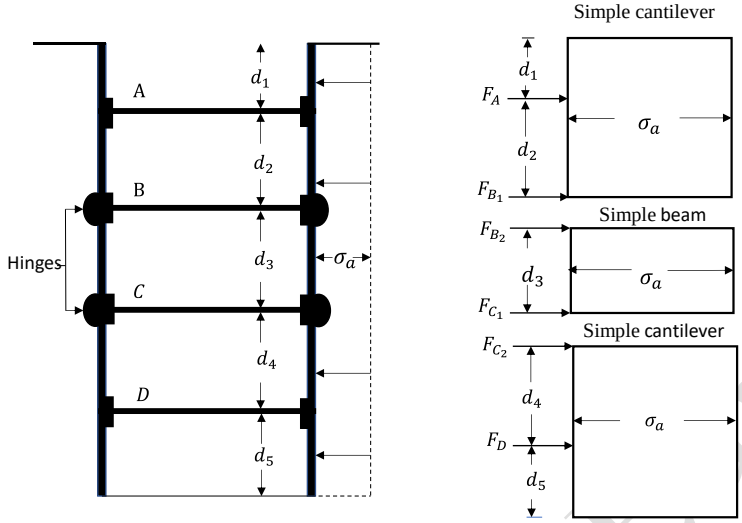

(a) (b)

Fig. 4 Braced Excavation System With 4 Struts

4.2. Monte Carlo Simulation (MCS)

The MCS method is a mathematical procedure for continuously evaluating an empirical operator having a random variable with known probability distribution (Liu et al. 2020). For obtaining the desired accuracy level of P_f, the number of samples to be generated by MCS should be at least equal to $10/P_f$ (Kim et al. 2000; Kar and Roy 2022). For illustration, to obtain P_f = 0.001 accuracy, the total number of samples to be generated by MCS should be at least equal to 10,000. The P_f of the Braced excavation is calculated as the ratio of the number of samples with FOS < 1.0 to the total number of generated samples. The P_f using MCS can determined using Eq. 11.

$$P_f = \frac{\text{Number of failed sample}}{\text{Total number of generated sample}} \quad (11)$$

4.3. Subset Simulation (SS)

The SS approach is an adaptive stochastic simulation process created for effectively estimating low levels of P_f. The fundamental idea behind SS is to represent low failure probabilities as products of smaller conditional failure probabilities, making it easier to estimate these smaller conditional probabilities with less computational effort (Au and Wang 2014; Gao et al. 2019; Tian et al. 2021). Detailed information regarding MCMC method is referring to Au and Wang (Au and Wang 2014). For any engineering system, P_f can be defined as the probability of FOS lower than f_s, i.e., $P_f = P(FOS < f_s)$. In accordance with SS, the P_f can be represented as shown in Eq. 12 (Au et al. 2010; Wang et al. 2011).

$$P_f = P(F_m) = P(F_1)\prod_{j=2}^{m} P(F_j \,|F_{j-1}) \quad (12)$$

where F_j = {FOS < fos_j, j = 1, 2, …, m} are a set of the failure events that occur in the intermediate stages, and they are specified by a succession of lowering the intermediate threshold values $fos_1 > fos_2 > \cdots, fos_m = fos$; P ($F_1$) = P (FOS < fos_1) and $P(F_j|F_{j-1})$ = P(FOS < $fos_j|fos_{j-1}$), j = 2, 3, …, m. During SS, the intermediate

threshold value $fos_1 > fos_2 > \cdots, fos_{m-1}$ are determined adaptively so that $P(F_1)$ and $P(F_j|F_{j-1})$, j = 2, 3… m – 1 always correspond to the specified conditional probability p_o.

5. Probabilistic analysis of Braced Excavation

To perform the PA, a package of worksheets and function Add-Ins in Excel called UPSS 3.0, a MS-Excel based platform integrating both MCS and SS based probabilistic simulation codes written in Visual Basic Programming language has been used. This platform was created by (Au and Wang 2014). The PA procedure using UPSS 3.0 comprises a few steps, namely: a) the development of a deterministic modelling (DM) worksheet for deterministic analysis of the problem under consideration, b) a uncertainty modelling (UM) worksheet that is used to create the random fields of the variables involved; c) a probabilistic modelling (PM) worksheet that is generated by linking the probabilistic parameters defined in the UM sheet with the DM sheet; and d) finally, a run sheet where the MCS and SS simulation are carried out. At the end of above following procedure, output is generated in the form of complimentary cumulative distribution function (CCDF) plots which are very useful in identifying the failure state of the system.

5.1. Random field generation procedure

In order to account for the possibility of random heterogeneity in soil shear strength parameters, it was hypothesised that the soil parameters (i.e., $c', \emptyset \; and \; \gamma$) would follow a lognormal distribution (Javankhoshdel and Bathurst 2016a; Touma 2018) with mean (μ) and variance (σ^2) of soil parameter. In this investigation, c' and γ are considered to be lognormally distributed along the depth of the vertical cut. Thus, $\ln c'$ and $\ln \gamma$ are lognormally distributed with mean $\mu_{\ln c'}$, variance $\sigma^2_{\ln c'}$ and $\mu_{\ln \gamma}$, variance $\sigma^2_{\ln \gamma}$ respectively. Eq. 13 shows the lognormal distribution of any random variable *x*, with a μ_x and σ_x in a lognormal field.

$$x = exp(\mu \bar{I} + \sigma \bar{L} \bar{\varepsilon}) \tag{13}$$

where, μ is the mean; σ is the standard deviation of x; $\bar{I}$ represents dimensional unit vector; $\bar{L}$ depicts the dimension lower triangular matrix and $\bar{\varepsilon}$ shows the dimensional standard Gaussian vector.

A correlation matrix $\bar{R}$ is developed in such a manner that satisfies $\bar{R} = \overline{LL^T}$. The correlation between ln $[x_{z_i}]$ and ln $[x_{z_j}]$ at a depth z_i and z_j represent as $R_{ij} = e\left(\frac{-2|z_i - z_j|}{\lambda}\right)$ where λ is the correlation length. The $\bar{\text{L}}$ represents the lower triangular matrix.

5.2. Material Cross Correlation Between Soil Parameters

The objective of the study is to analyse the relationship between cross-correlated random soil parameters (i.e., $c' \; and \; \gamma$) and the P_f during braced excavation procedure. To calculate the cross-correlation coefficient (ρ) between two correlated random variables X_i and X_j, expressed as ρ_{X_i,X_j} can be calculated using Eq. 14.

$$\rho = \rho_{X_i,X_j} = \frac{cvar_{X_iX_j}}{\sigma_{X_i}\sigma_{X_j}} \tag{14}$$

Here, σ_{X_i} and σ_{X_j} are the standard deviation of the random variables X_i and X_j respectively. $cvar_{X_iX_j}$ stands for the covariance of random variables X_i and X_j. For more detail on implementation of cross-correlation, one can refer to the literature (Javankhoshdel and Bathurst 2016b; Li et al. 2023). In this current work, the random variables c' and γ are expressed by the following Eqs. 15 and 16. In particular, the covariance matrix is given in Eq. 17.

$$c = \sigma_c Z + \mu_c \tag{15}$$

$$\gamma = \rho\sigma_\gamma Z + \sigma_\gamma\sqrt{1-\rho^2}Z + \mu_\sigma \quad (16)$$

$$\Lambda = \begin{bmatrix} {\sigma_c}^2 & \rho\sigma_c\sigma_\gamma \\ \rho\sigma_\gamma\sigma_c & {\sigma_\gamma}^2 \end{bmatrix} \quad (17)$$

6. Results and discussion

In this study, PA for a BES at a depth of cut 9.0 m was performed using MCS and SS with UPSS Add-ins 3.0 in MS Excel. For this, both deterministic and PA were conducted to compute the FOS against braced cut failure. The correlated spatially distributed random fields of c' and γ of soil following log-normal distribution along the depth using the concepts of Pearson Correlation matrix and Markov Correlation function. According to Table 1, the soil parameter c' was varied to have values of 10%, 30%, and 50% for both case-1 and case-2, while the value of γ was varied to have values of 5% and 7% respectively (Duncan 2000; Shahin and Cheung 2011).

Table. 1 Summary of COV of details soil parameters

		COV (%)			Range of COV	references
Case 1	c' (kN/m^2)	10	30	50	10% - 70%	(Shahin and Cheung 2011)
	γ(kN/m^3)	5	5	5	3% - 7%	(Michael 2000)
Case 2	c' (kN/m^2)	10	30	50	10% - 70%	(Shahin and Cheung 2011)
	γ(kN/m^3)	7	7	7	3% - 7%	(Michael 2000)

The "DM" worksheet (see Appendix Fig. 1A) used to conduct a deterministic analysis of the BES. The worksheet presents the analysis that has been performed for a braced cut at a depth of 9.0 m using four struts. The worksheet includes the calculation of strut force, design of sheet piles, and design of Wales. Notably, the resulting FOS calculation is based on the design of Wales.

The U.M worksheet was created using MS Excel by generating a $\bar{R}$ and $\bar{L}$ for soil parameters (i.e., c' and γ) at different depths. The U.M worksheet includes probability density functions (PDFs) and random values of cohesion and unit weights. Notably, this worksheet has been created separately for both with and without cross-correlation that has been presented in Appendix Fig. 2A and Fig. 3A, respectively. Note that, cross-correlation in between c' and γ was considered positive i.e., $\rho_{c',\gamma} = 0.1$. Also, it is note that, this study was analysed with correlation length of $\lambda = 1.0$ m and $\lambda = 2.0$ m. The U.M sheet consists of uniform i.i.ds generated by the RAND () function and standard normal variables generated using the NORMINV () function to convert i.i.ds to standard Gaussian variables. The random variables that are generated at various depths in the U.M. sheet is then averaged prior to being linked to the deterministic sheet, and the resulting worksheet is called the P.M sheet.

6.1. Selection of correlation coefficient

It has already been discussed that for cohesive soil, the soil parameters are positively correlated. In this study, distinct correlated coefficients (viz., 0.1, 0.3, 0.5, and 0.7) were investigated, and PA was performed using MCS. Fig. 5 deduced that the effect correlated coefficient on P_f. This plot has been plotted considering specific FOS and their corresponding P_f. As the value of ρ decreases, P_f increases for a constant value of FOS. However, increasing the value of ρ has a very low effect on P_f. The correlation coefficient $\rho_{c',\gamma} = 0.10$ has been chosen because the maximum P_f of the braced excavation system has been reported in this paper.

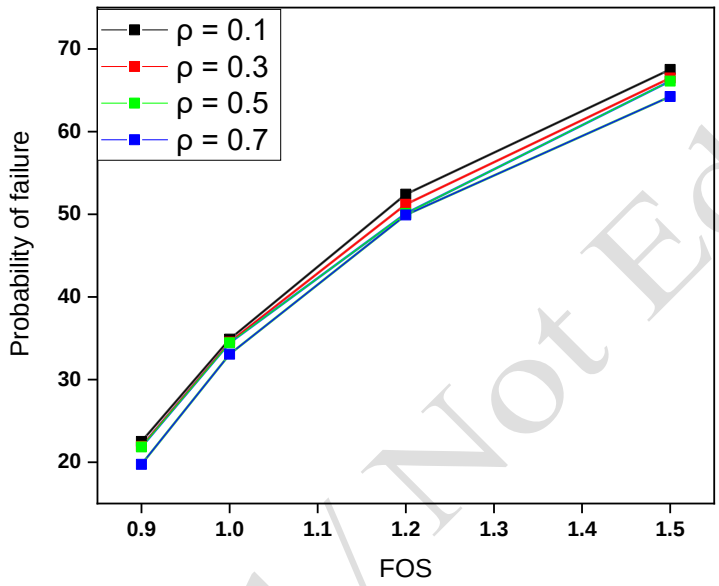

Fig. 5 Plot in between P_f and FOS at different value of correlation coefficient

6.2. MCS Analysis Results

Table 3 displays the results of a 10,000-sample MCS analysis for the braced excavation system. The simulations were conducted for correlating length of $\lambda = 1.0$ m and $\lambda = 2.0$ m, at depths of cut 9.0 m, respectively. The data shows that P_f of the braced excavation system increases when COV of c' and γ are increased. Furthermore, it is seen that P_f value increases when λ increases. Also, it is noticed that if the cross-correlation between c' and γ is considered, there is further increase in P_f of the system. Therefore, considering the correlated structure of related variables is crucial to ensure conservative results. For clarity, CCDF plot in Fig. 6 (uncorrelated) and Fig. 7 (correlated) has been presented. It can be seen from the CCDF, as the COV value increases, the curve of the CCDF plot shift to the right, indicating more failure. Fig. 8 and Fig. 9 show histograms for the worst-case scenario $\nu_{c'} = 50\%$ and $\nu_{\gamma} = 5\%$ using MCS, with and without correlation, at a depth of cut 9.0 m for λ= 2.0 m. Herein, notation $\nu_{c'}$ indicates the COV of cohesion and ν_{γ} indicates the COV of unit weight. In Fig. 8, among 10,000 samples, 3487 had FOS values below one (FOS < 1). Therefore, the P_f was calculated as $\left(\frac{3487}{10000}\right) \times 100 = 34.87\%$, and the resolution of P_f was determined to be $\left(\frac{1}{10000}\right) \times 100 = 0.01\%$.

Table 3 Results obtained from MCS at a depth of cut 9.0 m

Correlation length, λ	COV, c (%)	COV, γ (%)	Number of samples generated	Number of failed samples having FOS<1 when ρ = 0.0	Number of failed samples FOS<1 when ρ = 0.1	P_f (%) for ρ = 0.0	P_f (%) for ρ = 0.1
$\lambda = 1$	10	5	10000	0	294	0	2.94
	30	5	10000	78	2456	0.78	24.56
	50	5	10000	994	3452	9.94	34.52
	10	7	10000	0	385	0	3.85
	30	7	10000	13	2390	0.13	23.90
	50	7	10000	807	3439	8.07	34.39
$\lambda = 2$	10	5	10000	0	314	0	3.14
	30	5	10000	202	2523	2.02	25.23
	50	5	10000	1551	3487	15.51	34.87
	10	7	10000	0	394	0	3.94
	30	7	10000	90	2530	0.9	25.30
	50	7	10000	1335	3480	13.35	34.80

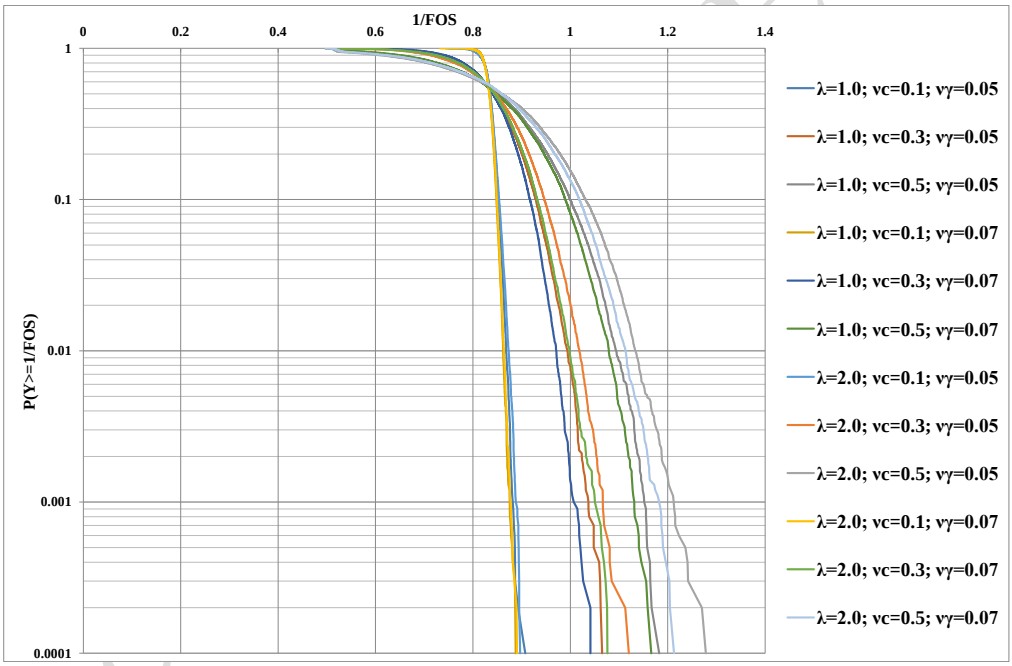

Fig. 6 CCDF plot between P_f and 1/FOS using MCS at a depth of cut 9.0 m (without correlation)

6.3. Comparative study for with and without cross-correlation in MCS

Comparing the results of the simulations with and without cross-correlation using MCS, it was found that the P_f increases significantly when cross-correlation (Viz., $\rho_{c',\gamma} = 0.1$) was considered. It can be deduced from Table. 3, there have not been obtained any failed sample in a system, when $\nu_{c'}$ = 10% and ν_{γ} = 5%, and $\nu_{c'}$ = 10% and ν_{γ} = 7% with correlation length of $\lambda = 1.0$ m and $\lambda = 2.0$ m are considered. However, when cross-correlation was considered, a significant number of failed samples were observed at $\lambda = 1.0$ m and $\lambda = 2.0$ m.

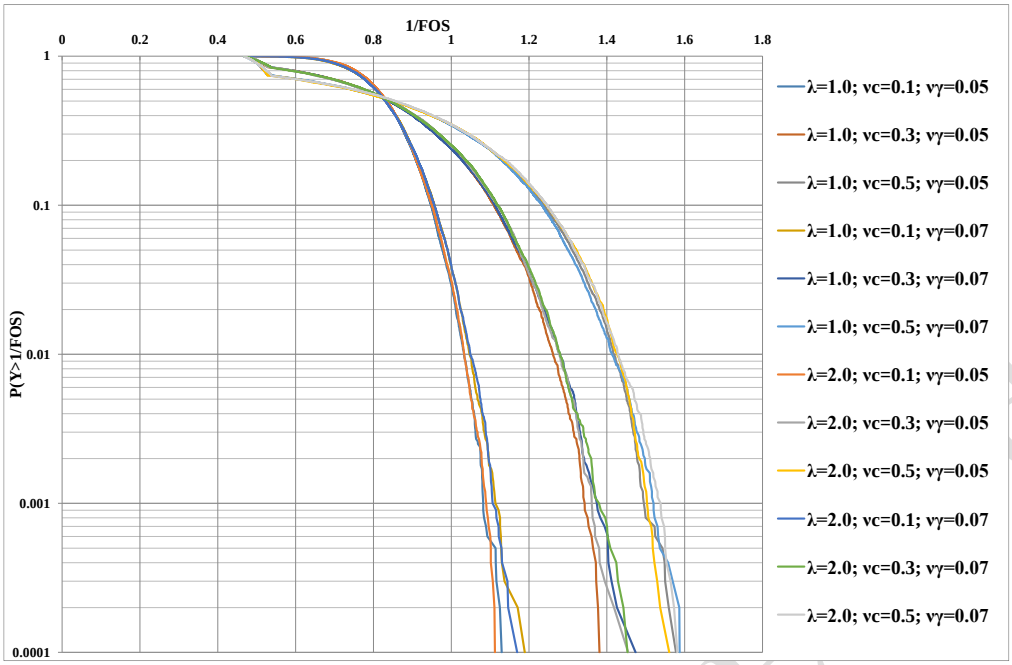

Fig. 7 CCDF plot between P_f and 1/FOS using MCS at a depth of cut 9m (with correlation)

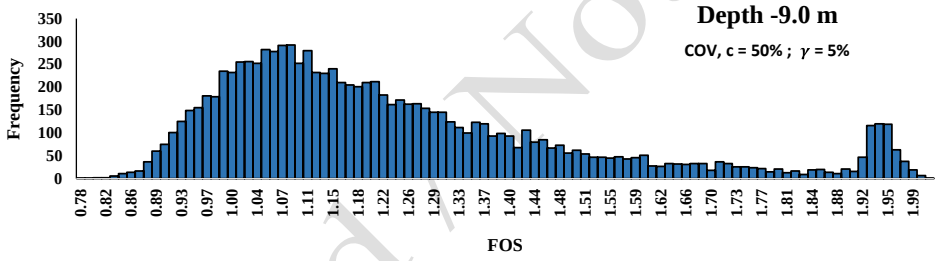

Fig. 8 Histogram at a depth of cut 9.0 m at $\lambda = 2.0$ m (without correlation)

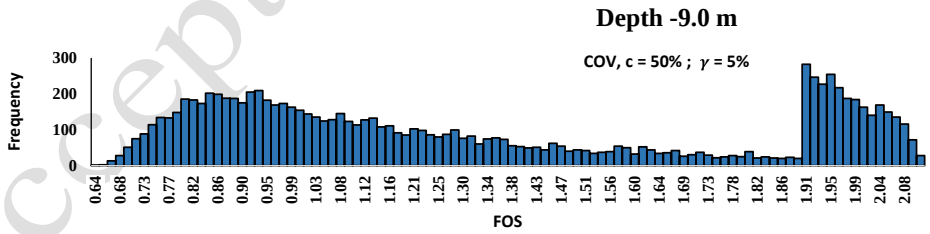

Fig. 9 Histogram at a depth of cut 9 m at $\lambda = 2.0$ m (with correlation)

6.4. SS Analysis results

In this study, SS was used with 1400 random samples distributed across three simulation stages (levels 1, 2, and 3) with 1 run, N = 500, and $p_0 = 0.1$. The total number of samples is calculated as $N + m \times (1 - p_0)$ i.e., 500 + 3*(1 – 0.1) = 1400. As an example, when λ = 1.0 m and ρ = 0.0, in the third row of Table 3, there were 5, 450, and 500 failures in levels 1, 2, and 3, respectively. The probability of occurrence at levels 1, 2, and 3 is 0.9, 0.09, and 0.01, respectively. Therefore, P_f can be found using Eq. 12 as $\left(0.9 \times \frac{5}{450} + 0.09 \times \frac{450}{450} + 0.01 \times \frac{500}{500}\right) \times 100 = 11\%$.

Table 4 displays the results of an SS analysis for the BES using 1400 samples. This simulation shows that P_f of the BES increases when $\nu_{c'}$ and ν_γ are increased. Furthermore, it is seen that P_f value increases when λ increases. Additionally, it is noted that the system's P_f continues to rise when the cross-correlation between c' and γ is taken into account. The results show that SS provides similar outcomes to MCS with fewer random samples needed. CCDF plots in Fig. 10 and Fig. 11 depict SS results at various COV levels with ρ = 0 and ρ = 0.1 for a 9.0 m cut depth. Histogram plots (Fig. 12 and Fig. 13) for the worst-case P_f scenario at a 9.0 m cut depth are presented using SS. The presented histograms clearly show failures at each simulation level. In Fig. 12, out of 1400 samples, 29 failed at level-1, and all samples failed at level-2 and level-3.

Table 4. Results of SS at depths of cut of 9.0 m (with cross correlation)

Correlation, λ	$\nu_{c'}$(%)	ν_γ(%)	Total Samples Produced	Number of failed samples having FOS<1 when ρ = 0.0			Number of failed samples having FOS<1 when ρ = 0.1			P_f(%) for ρ = 0	P_f(%) for ρ = 0.1
				Level 1	Level 2	Level 3	Level 1	Level 2	Level 3		
$\lambda = 1$	10	5	1400	0	0	0	0	110	500	0	3.2
	30	5	1400	0	7	500	75	450	500	1.14	25
	50	5	1400	5	450	500	123	450	500	11	34.6
	10	7	1400	0	0	0	0	155	500	0	4.32
	30	7	1400	0	0	85	79	450	500	0.17	25.8
	50	7	1400	0	386	500	125	450	500	8.72	35
$\lambda = 2$	10	5	1400	0	0	0	0	113	500	0	3.26
	30	5	1400	0	96	500	82	450	500	2.92	26.4
	50	5	1400	29	450	500	126	450	500	15.8	35.2
	10	7	1400	0	0	0	0	180	500	0	4.6
	30	7	1400	0	0	477	84	450	500	0.95	26.8
	50	7	1400	24	450	500	130	450	500	14.8	36

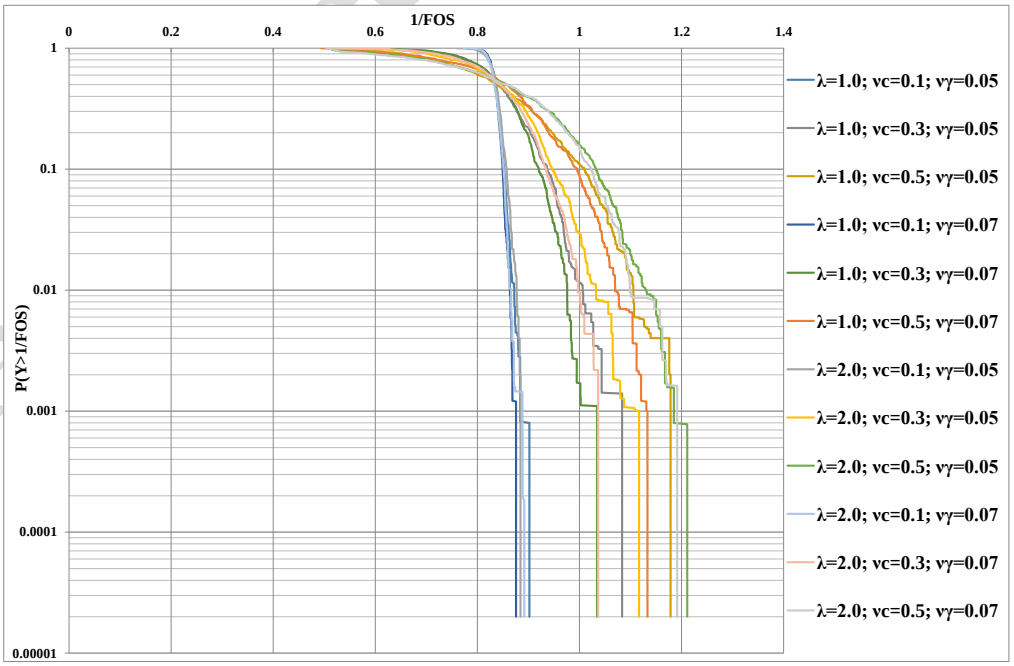

Fig. 10 CCDF plot between P_f and 1/FOS using SS at a depth of cut 9.0 m (without cross-correlation)

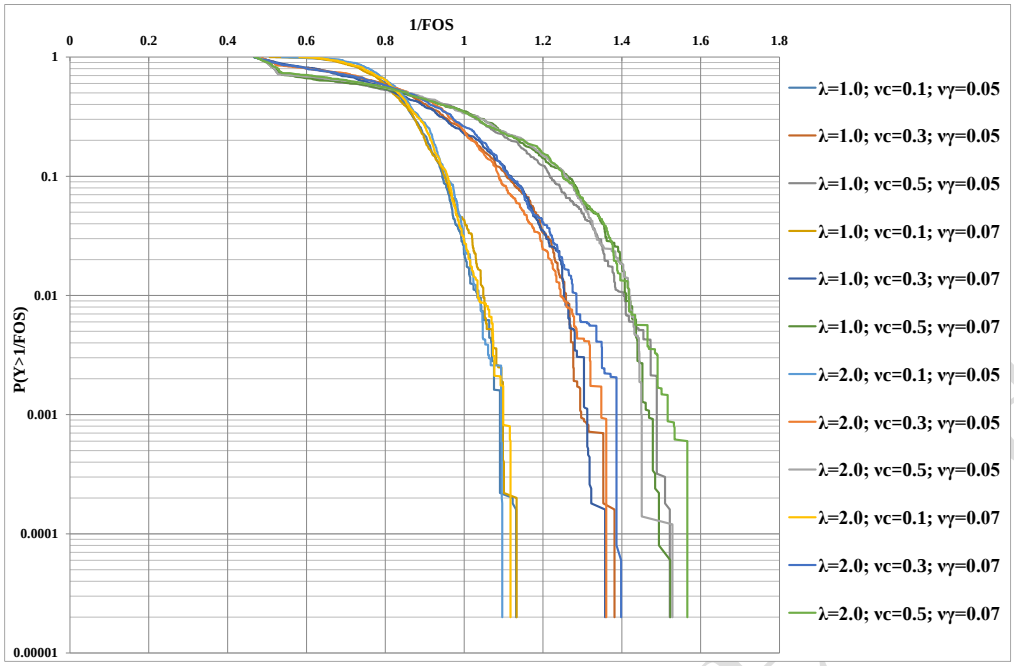

Fig. 11 CCDF plot between P_f and 1/FOS using SS at a depth of cut 9m (with cross-correlation)

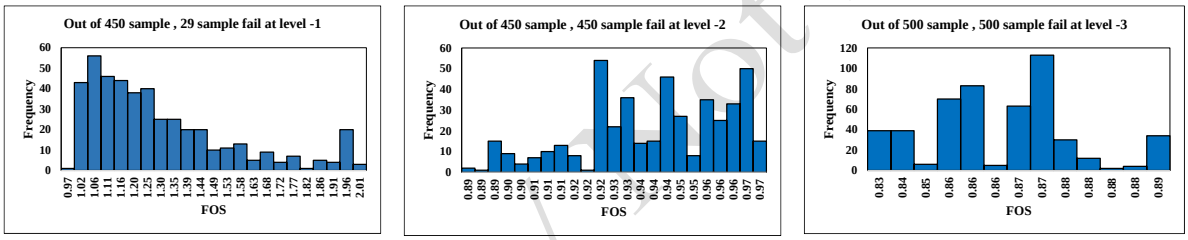

Fig. 12 Histogram plot in SS for worst P_f condition (without correlation)

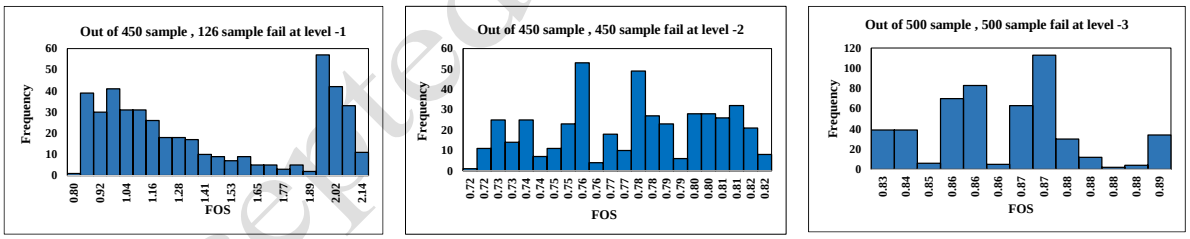

Fig. 13 Histogram plot using SS for worst P_f condition (with cross-correlation)

6.5. Comparative study with and without cross-correlation in SS

Table 4 shows no failures at any level when $\nu_{c'}$ was 10% and ν_{γ} was 5% and 7% for both λ = 1.0 m and λ = 2.0 m. In Table 3 (row 1), considering the same COVs for soil parameters but accounting for cross-correlation between c' andγ, 110 samples failed at level 2 and 500 samples failed at level 3 for λ = 1.0 m. This suggests that incorporating cross-correlation between c' and γ leads to an increase in the P_f.

6.6. Computational Cost of SS over MCS

This section discusses the comparative analysis between the employed MCS and SS simulation in terms of cost. In this study, we utilized the UPSS 3.0 Spreadsheet environment, which is open source. For the simulation analysis, we operated on a 64-bit operating system with an x64-based processor, CPU @ 2.40GHz, and 8.00 GB RAM.

To get the same level of probability, SS demonstrates advantages in efficiency over direct Monte Carlo Simulation (MCS) for achieving comparable levels of probability. Specifically, SS requires a smaller sample size, resulting computation time of 16.37 seconds across three levels of simulation. In contrast, MCS required 1.20 minutes for the same analysis. On the other hand, MCS requires high computational cost and time, if greater number of samples are used for simulation.

7. Summary and conclusion

The current study primarily emphasises conducting a PA of a braced excavation by utilising a spreadsheet version of Microsoft Excel to perform MCS and SS simulations. In this work, PA for braced cuts was carried out at a depth of cut 9.0 m utilizing four struts. For this, the soil parameter c' and γ were considered as uncertain parameters and modelled with lognormal random field and Cholesky lower triangular matrix were created. In addition, four different correlation coefficient values between soil parameters (i.e., c' and γ) on the response P_f were investigated. Based on the results obtained on P_f, the best correlation coefficient (i.e., $\rho = 0.1$) were considered for this investigation. Furthermore, the comparative analysis was conducted to investigate the effects of braced excavation at various depths, utilizing techniques such as MCS and SS to evaluate the P_f. Additionally, the study examined various levels of COV and varied soil parameters c' to 10%, 30%, and 50%, while also altering the γ to 5% and 7%. Based on obtained results in this investigation following conclusion can be drawn:

i. Four different correlation coefficients (viz., 0.1, 0.3, 0.5, and 0.7) were investigated and probabilistic analysis were conducted by both MCS and SS methods. It is seen that ρ = 0.10 yields maximum P_f for box drain system.

ii. It is seen that the consideration of correlation between the soil parameters (i.e., c' and γ) yields higher P_f value compared to the situation when the soil parameters are deemed uncorrelated.

iii. When correlation length is increased in both MCS and SS, the P_f increases dramatically.

iv. When MCS and SS are conducted for probabilistic analysis, then it found that SS are superior at low level of failure. In addition, obtained results by SS was approximately similar to those obtained MCS which also shows that both of the methods are applicable for probabilistic analysis.

v. SS requires a smaller number of samples to report P_f with same level of accuracy as MCS. This fact indicates that SS has better efficiency than MCS in terms of both memory storage space and computational time.

DETERMINISTIC MODELLING SHEET

Π (pi)	Excavation height (H)	Depth of 1st strut (from GL)	Depth of 2nd strut (from GL)	Depth of 3rd strut (from GL)	Depth of 4th strut (from GL)	Allowable Stress in Strut (σ_{all})	Width of the Cut (B)	Length of the Cut (L)	Thickness of Clay below the base of excavation (T)	Height of the Cut (H)	Surcharge load =
3.142	9	1.6	3.5	5.5	7.4	170000	11	20	9	9	40
	m	m	m	m	m	kN/m^2	m	m	m	m	kN/m^2

PART A — **APPERENT EARTH PRESSURE DIAGRAM:**

ϒH/C > 4	σ_a = greater of 0.3*ϒ*H and ϒH(1-(4C/ϒH))		m_1	Check Satisfaction
10.6875	107	kN/m^2	47.55555556	YES

SOIL INPUT DATA:

ϒ =	19	kN/m^3
C =	16	kN/m^2
ϕ =	0	Degrees

PART B — **STRUT FORCE CALCULATION:**

Strut reaction at A, (F_A) =	Strut reaction at B, (F_B) =	Strut reaction at C, (F_C) =	Strut reaction at D (F_D) =
170.707	190.418	136.566	344.934
kN/m	kN/m	kN/m	kN/m
Strut Spacing , s =	Total Strut Load, P_A =	Total Strut Load, P_B =	Total Strut Load, P_C =	Total Strut Load, P_D =
3	512.122	571.253	409.697	1034.803
m	kN	kN	kN	kN

		kN/m	
$\sum M_B = 0$	F_A =	170.707	
$\sum Fv = 0$	F_{B1} =	83.418	
$\sum Fv = 0$	F_{B2} =	107	
$\sum M_C = 0$	F_D =	344.934	
$\sum Fv = 0$	F_{C1} =	107	
$\sum Fv = 0$	F_{C2} =	29.566	
	F_B =	190.418	
	F_c =	136.566	

Overhanging lenth before,	L_u =	1.6 m
Distance b/w 1st and 2nd strut,	L_1 =	1.9 m
Distance b/w 2nd and 3rd strut,	L_2 =	2 m
Distance b/w 3rd and 4th strut,	L_3 =	1.9 m
Distance b/w 3rd and dredge level,	L_d =	1.6 m
Check:		
Total Load on the span =		842.625 kN/m
Sum of all reaction forces =		842.625 kN/m

PART C — **Section modulus of sheet pile:**

Span AB and Overhang	Load amount at the postion of 1st strut =	76.089	kN/m^2
	Location of Point E is x_1 =	0.780	m
	Negative B.M. at A = M_A =	-32.465	kN-m per m of wall
	Moment at E, M_E =	32.516	kN-m per m of wall
	Negative S.F. at location of 1st strut =	-60.871	kN/m
	Positive S.F. at location of 1st strut =	109.836	kN/m
	S.F. at the location of 0.25H =	50.332	kN/m
	Negative S.F. at location of 2nd strut =	-83.418	kN/m
	Positive S.F. at location of 2nd strut =	0.000	kN/m
	Net Positive S.F. at location of 2nd strut =	107.000	kN/m
Span BC			
	Positive S. F. at the location of 2nd strut at B =	107.000	kN/m
	Negative S. F. at the location of 3rd strut at C =	-107	kN/m
	Positive S. F. at the location of 3rd strut at C =	136.566	kN/m
	Positive B.M. at the middle of span =	53.5	kN-m per m of wall
Span CD and Overhang	Location of Point F is x_2 =	0.276	m
	Magnitude of negative B.M. at 4th strut location D (M_D)=	-136.96	kN-m per m of wall
	Magnitude of moment at F, (M_F) =	4.085	kN-m per m of wall
	M_{max} =	136.96	kN-m per m of wall
	Allowable Stress in Strut (σ_{all}) =	170000	kN/m^2
	Section Modulus of sheet pile (S) =	0.000805647	m^3/m per m of wall

PART D — **Section modulus of wales:**

The reaction at level B is calculated in Part B. Therefore,		
Maximum moment at 1st strut level = A*s^2/8 =	192.046	kN-m
Maximum moment at 2nd strut level = M_{max} = (B1+B2)*s^2/8 =	214.220	kN-m
Maximum moment at 3rd strut level = C*s^2/8 =	153.637	kN-m
Maximum moment at 4th strut level = D*s^2/8 =	388.051	kN-m
Overall Maximum moment (Mmax) =	388.051	kN-m
Wales Section Modulus , S =	0.002282653	m^3
	2282.652864	cm^3
Allowable section modulus=	2000	cm^3
F.S of wales=	0.876173522	

Fig. 1A Deterministic modelling sheet of Braced cut

UNCERTAINTY MODELLING SHEET

λ = 1.0 m

Parameter 1 :Cohesion

Parameter 2 :Bulk Density

Depth (z in m)	Mean(μ)	Std. Deviation(σ)	COV	Lognormal Mean	Lognormal Std.Deviation	C'	$(\mu_{c'})$	$(\mu_{lnc'})$	$(\sigma_{c'})$	$(\sigma_{lnc'})$	Mean(μ)	Std. Deviation (σ)	COV	Lognormal Mean	Lognormal Std.Deviation	Y'	$(\mu_{Y'})$	$(\mu_{lnY'})$	$(\sigma_{Y'})$	$(\sigma_{lnY'})$	Z1	Z2
0	11	1.1	0.1	2.39292	0.09975	2.38775	10.88900	2.38268	1.1	0.10076	16.625	0.83125	0.05	2.80966	0.04997	2.81616	16.71250	2.81492	0.83125	0.04971	0.479351	0.554036
1	11	1.1	0.1	2.39292	0.09975	2.38775	10.88900	2.38268	1.1	0.10076	16.78833	0.83942	0.05	2.81944	0.04997	2.82593	16.87669	2.82470	0.83942	0.04971	-0.0518	0.1359
2	11.3333	1.13333	0.1	2.42277	0.09975	2.41760	11.21894	2.41253	1.13333	0.10076	16.95167	0.84758	0.05	2.82912	0.04997	2.83562	17.04089	2.83438	0.84758	0.04971		
3	12	1.2	0.1	2.47993	0.09975	2.47476	11.87891	2.46969	1.2	0.10076	17.115	0.85575	0.05	2.83871	0.04997	2.84520	17.20508	2.84397	0.85575	0.04971	ρ =	0.1
4	20	2	0.1	2.99076	0.09975	2.98559	19.79818	2.98051	2	0.10076	17.605	0.88025	0.05	2.86693	0.04997	2.87343	17.69766	2.87220	0.88025	0.04971		
5	23.3333	2.33333	0.1	3.14491	0.09975	3.13974	23.09784	3.13466	2.33333	0.10076	17.44167	0.87208	0.05	2.85761	0.04997	2.86411	17.53347	2.86288	0.87208	0.04971		
6	22	2.2	0.1	3.08607	0.09975	3.08090	21.77800	3.07582	2.2	0.10076	17.605	0.88025	0.05	2.86693	0.04997	2.87343	17.69766	2.87220	0.88025	0.04971	Cavg	20.3858
7	24.66667	2.466667	0.1	3.20048	0.09975	3.19531	24.41776	3.19023	2.466667	0.10076	17.76833	0.88842	0.05	2.87617	0.04997	2.88267	17.86185	2.88143	0.88842	0.04971	Yavg	17.5892
8	26.16667	2.616667	0.1	3.25951	0.09975	3.25434	25.90262	3.24927	2.616667	0.10076	17.85	0.8925	0.05	2.88076	0.04997	2.88725	17.94395	2.88602	0.8925	0.04971		
9	26.5	2.65	0.1	3.27217	0.09975	3.26700	26.23259	3.26193	2.65	0.10076	17.85	0.8925	0.05	2.88076	0.04997	2.88725	17.94395	2.88602	0.8925	0.04971		

Random Sample generation

Vertical Depth	0	1	2	3	4	5	6	7	8	9
Uniform I.I.D.	0.75458	0.48464	0.38154	0.46267	0.04949	0.98182	0.38213	0.58502	0.95545	0.62737
Std. Normal I.I.D. (Z)	0.689	-0.0385	-0.3014	-0.0937	-1.6498	2.0929	-0.2999	0.2148	1.7002	0.3249
PDF Value p(Z)	0.3146	0.3986	0.3812	0.3972	0.1023	0.0446	0.3814	0.3898	0.094	0.3277
L*Z	0.677577102	-0.08363	-0.33607	-0.27667	-1.35832	2.04161	-0.23669	0.44670	1.72812	0.32191
$lnc'=\mu_{lnc'}+\sigma_{lnc'}*L*Z$	2.45534	2.37941	2.38408	2.44717	2.85010	3.34339	3.05729	3.23987	3.42673	3.29911
$c'=$	11.65000	10.79854	10.84907	11.55556	17.28944	28.31503	21.26985	25.53039	30.77574	27.08861
$lnY'=\mu_{lnY'}+\sigma_{lnY'}*L*Z$	2.85001	2.82175	2.81882	2.83138	2.80556	2.96613	2.86161	2.90499	2.97361	2.90334
Y'	17.29000	16.80631	16.75711	16.96886	16.53631	19.41660	17.48958	18.26503	19.56232	18.23492

Cholesky Transformation Matrix Written and Computed by Matlab

	0	1	2	3	4	5	6	7	8	9
0	1	0	0	0	0	0	0	0	0	0
1	0.13534	1	0	0	0	0	0	0	0	0
2	0.01832	0.13409	1	0	0	0	0	0	0	0
3	0.00248	0.01815	0.13409	1	0	0	0	0	0	0
4	0.00034	0.00246	0.01815	0.13409	1	0	0	0	0	0
5	4.54E-05	0.00033	0.00246	0.01815	0.13409	1	0	0	0	0
6	6.14E-06	4.50E-05	0.00033	0.00246	0.01815	0.13409	1	0	0	0
7	8.32E-07	6.09E-06	4.50E-05	0.00033	0.00246	0.01815	0.13409	1	0	0
8	1.13E-07	8.24E-07	6.09E-06	4.50E-05	0.00033	0.00246	0.01815	0.13409	1	0
9	1.52E-08	1.11E-07	8.24E-07	6.09E-06	4.50E-05	0.00033	0.00246	0.01815	0.13409	1

Fig. 2A Uncertainty model worksheet with cross-correlation

UNCERTAINTY MODELLING SHEET

Depth (z in m)	0	1	2	3	4	5	6	7	8	9
Correlation length	1	1	1	1	1	1	1	1	1	1
Parameter 1 :Cohesion										
Mean of Cohesion (KN/m^2)	11.00	11.00	11.33	12.00	20.00	23.33	22.00	24.67	26.17	26.50
Std dev of Cohesion	1.10	1.10	1.13	1.20	2.00	2.33	2.20	2.47	2.62	2.65
C.O.V	0.1	0.1	0.1	0.1	0.1	0.1	0.1	0.1	0.1	0.1
Mean of ln(C)	2.393	2.393	2.423	2.480	2.991	3.145	3.086	3.200	3.260	3.272
Std dev of ln(C)	0.100	0.100	0.100	0.100	0.100	0.100	0.100	0.100	0.100	0.100
Parameter 2 :Bulk Density										
Yb (KN/m^2)	16.625	16.788	16.952	17.115	17.605	17.442	17.605	17.768	17.850	17.850
Std dev of Yb	0.831	0.839	0.848	0.856	0.880	0.872	0.880	0.888	0.893	0.893
C.O.V	0.050	0.050	0.050	0.050	0.050	0.050	0.050	0.050	0.050	0.050
ln(Yb)	2.810	2.819	2.829	2.839	2.867	2.858	2.867	2.876	2.881	2.881
Std dev of ln (Yb)	0.050	0.050	0.050	0.050	0.050	0.050	0.050	0.050	0.050	0.050

Generation of lognormal field for cohesion and unit weight by cholesky transformatoion

LN(cohesion)	2.442	2.307	2.371	2.358	3.063	3.069	3.096	3.209	3.319	3.265
Cohesion (KN/m^2)	11.491	10.047	10.706	10.570	21.389	21.530	22.100	24.765	27.629	26.185
Cavg (KN/m^2)	19.43563									
LN(Yb)	2.8340	2.7765	2.8031	2.7776	2.9031	2.8198	2.8717	2.8807	2.9105	2.8773
Yb (KN/m^3)	17.0136	16.0631	16.4953	16.0811	18.2297	16.7736	17.6671	17.8261	18.3658	17.7654
Ybavg (KN/m^3)	17.2717									

Random Sample generation

Depth	0.000	1.000	2.000	3.000	4.000	5.000	6.000	7.000	8.000	9.000
Uniform I.I.D	0.727	0.213	0.360	0.091	0.798	0.219	0.533	0.504	0.729	0.472
Std normal I.I.D (z)	0.605	-0.796	-0.359	-1.332	0.833	-0.777	0.084	0.010	0.610	-0.071
Pdf value p(z)	0.332	0.291	0.374	0.164	0.282	0.295	0.398	0.399	0.331	0.357
L*Z	0.487	-0.859	-0.521	-1.222	0.723	-0.757	0.095	0.090	0.595	-0.070

Cholesky Transformation Matrix Written and Computed by Matlab

	0	1	2	3	4	5	6	7	8	9
0	1	0	0	0	0	0	0	0	0	0
1	0.135335	1	0	0	0	0	0	0	0	0
2	0.018316	0.13409	1	0	0	0	0	0	0	0
3	0.002479	0.018147	0.13409	1	0	0	0	0	0	0
4	0.000335	0.002456	0.018147	0.13409	1	0	0	0	0	0
5	4.54E-05	0.000332	0.002456	0.018147	0.13409	1	0	0	0	0
6	6.14E-06	4.50E-05	0.000332	0.002456	0.018147	0.13409	1	0	0	0
7	8.32E-07	6.09E-06	4.50E-05	0.000332	0.002456	0.018147	0.13409	1	0	0
8	1.13E-07	8.24E-07	6.09E-06	4.50E-05	0.000332	0.002456	0.018147	0.13409	1	0
9	1.52E-08	1.11E-07	8.24E-07	6.09E-06	4.50E-05	0.000332	0.002456	0.018147	0.13409	1

Fig. 3A Uncertainty model worksheet without cross-correlation

Authorship contribution:

Pratima Kumari: Conceptualization, Data curation, Formal analysis, Investigation, Methodology, Resources, Visualization, Writing – original draft

Pijush Samui: Supervision

Avijit Burman: Supervision

Declaration of Competing Interest:

The authors affirm that there is no known financial or interpersonal dispute that might have appeared to have influenced the research presented in this paper.

Funding:

No external funding has been received.

Data availability:

The dataset used in this study is available upon request. Please contact to corresponding author for access to the data.

References

Ahmad F, Samui P, Mishra SS (2024) Probabilistic slope stability analysis using subset simulation enhanced by ensemble machine learning techniques. Model Earth Syst Environ 10:2133–2158. https://doi.org/10.1007/s40808-023-01882-4

Au S-K, Wang Y (2014) Engineering risk assessment with subset simulation. John Wiley & Sons

Au SK, Cao ZJ, Wang Y (2010) Implementing advanced Monte Carlo simulation under spreadsheet environment. Struct Saf 32:281–292. https://doi.org/10.1016/j.strusafe.2010.03.004

Bahrami M (2019) Strut Design of Deep Excavation: Theory and Solved Example. SSRN Electron J. https://doi.org/10.2139/ssrn.3486532

Cho SE, Park HC (2010) Effect of spatial variability of cross-correlated soil properties on bearing capacity of strip footing. Int J Numer Anal Methods Geomech 34:1–26. https://doi.org/10.1002/nag.791

Chowdhury SS (2017) Reliability Analysis of Excavation Induced Basal Heave. Geotech Geol Eng 35:2705–2714. https://doi.org/10.1007/s10706-017-0272-2

Dan K, Sahu RB (2022) Effect of arching on active earth pressure distribution against braced wall. Int J Geotech Eng 16:826–837. https://doi.org/10.1080/19386362.2021.1912921

Duncan JM (2000) Factors of safety and reliability in geotechnical engineering. J Geotech geoenvironmental Eng 126:307–316

Farzi M, Pakbaz MS, Aminpour HA (2018) Selection of support system for urban deep excavations: A case study in Ahvaz geology. Case Stud Constr Mater 8:131–138. https://doi.org/10.1016/j.cscm.2018.01.004

Gao G-H, Li D-Q, Cao Z-J, et al (2019) Full probabilistic design of earth retaining structures using generalized subset simulation. Comput Geotech 112:159–172. https://doi.org/https://doi.org/10.1016/j.compgeo.2019.04.020

Han M, Chen X, Li Z, Jia J (2023) Improved inverse analysis methods and modified apparent earth pressure for braced excavations in soft clay. Comput Geotech 159:105456. https://doi.org/https://doi.org/10.1016/j.compgeo.2023.105456

He L, Liu Y, Bi S, et al (2020) Estimation of failure probability in braced excavation using Bayesian networks with integrated model updating. Undergr Sp 5:315–323.

https://doi.org/https://doi.org/10.1016/j.undsp.2019.07.001

Javankhoshdel S, Bathurst RJ (2016a) Influence of cross correlation between soil parameters on probability of failure of simple cohesive and c -ϕ slopes. Can Geotech J 53:839–853. https://doi.org/10.1139/cgj-2015-0109

Javankhoshdel S, Bathurst RJ (2016b) Influence of cross correlation between soil parameters on probability of failure of simple cohesive and c-ϕ slopes. Can Geotech J 53:839–853

Juang CH, Zhang J, Shen M, Hu J (2019) Probabilistic methods for unified treatment of geotechnical and geological uncertainties in a geotechnical analysis. Eng Geol 249:148–161

Kar SS, Roy LB (2022) Probabilistic based reliability slope stability analysis using FOSM, FORM, and MCS. Eng Technol Appl Sci Res 12:8236–8240

Kim H, Robert CP, Casella G (2000) Monte Carlo Statistical Methods. Technometrics 42:430. https://doi.org/10.2307/1270959

Lee TW, Kwak BM (1987) A Reliability-Based Optimal Design Using Advanced First Order Second Moment Method. Mech Struct Mach 15:523–542. https://doi.org/10.1080/08905458708905132

Li Y, Zhang F, Yeh T-CJ, et al (2023) Cross-Correlation Analysis of the Stability of Heterogeneous Slopes. Water 15

Liu X, Li D-Q, Cao Z-J, Wang Y (2020) Adaptive Monte Carlo simulation method for system reliability analysis of slope stability based on limit equilibrium methods. Eng Geol 264:105384. https://doi.org/https://doi.org/10.1016/j.enggeo.2019.105384

Low BK (2021) Reliability-Based Design in Soil and Rock Engineering. CRC Press, Boca Raton

Luo Z, Atamturktur S, Cai Y, Juang CH (2012) Simplified Approach for Reliability-Based Design against Basal-Heave Failure in Braced Excavations Considering Spatial Effect. J Geotech Geoenvironmental Eng 138:441–450. https://doi.org/10.1061/(ASCE)GT.1943-5606.0000621

Luo Z, Das BM (2016) System probabilistic serviceability assessment of braced excavations in clays. Int J Geotech Eng 10:135–144. https://doi.org/10.1179/1939787915Y.0000000021

Luo Z, Hu B, Wang Y, Di H (2018) Effect of spatial variability of soft clays on geotechnical design of braced excavations: A case study of Formosa excavation. Comput Geotech 103:242–253. https://doi.org/10.1016/j.compgeo.2018.07.020

Michael DJ (2000) Factors of Safety and Reliability in Geotechnical Engineering. J Geotech Geoenvironmental Eng 126:307–316. https://doi.org/10.1061/(ASCE)1090-0241(2000)126:4(307)

Nguyen VU, Chowdhury RN (1985) Simulation for risk analysis with correlated variables. Géotechnique 35:47–58. https://doi.org/10.1680/geot.1985.35.1.47

Peck BB (1969) Deep excavation and tunnelling in soft ground, State of the art volume. In: 7th ICSMFE. pp

225–290

Qi X-H, Zhou W-H (2017) An efficient probabilistic back-analysis method for braced excavations using wall deflection data at multiple points. Comput Geotech 85:186–198. https://doi.org/10.1016/j.compgeo.2016.12.032

Sabri MS, Ahmad F, Samui P (2024) Machine Learning-Aided Monte Carlo Simulation and Subset Simulation. Transp Res Rec 03611981241248166. https://doi.org/10.1177/03611981241248166

Sekhavatian A, Janalizadeh Choobbasti A (2018a) Comparison of Point Estimate and Monte Carlo probabilistic methods in stability analysis of a deep excavation. Int J Geo-Engineering 9:20. https://doi.org/10.1186/s40703-018-0089-8

Sekhavatian A, Janalizadeh Choobbasti A (2018b) Reliability analysis of deep excavations by RS and MCS methods: case study. Innov Infrastruct Solut 3:60. https://doi.org/10.1007/s41062-018-0166-z

Shahin MA, Cheung EM (2011) Stochastic design charts for bearing capacity of strip footings. Geomech Eng 3:153–167. https://doi.org/10.12989/gae.2011.3.2.153

Sivakugan N, Das BM (2009) Geotechnical engineering: a practical problem solving approach. J. Ross Publishing

Terzaghi K, Peck RB, Mesri G (1996) Soil mechanics in engineering practice. John wiley & sons

Tian H-M, Li D-Q, Cao Z-J, et al (2021) Reliability-based monitoring sensitivity analysis for reinforced slopes using BUS and subset simulation methods. Eng Geol 293:106331. https://doi.org/https://doi.org/10.1016/j.enggeo.2021.106331

Touma D (2018) From Ground Measurements to Global Models: Temporal and Spatial Characteristics of Drought and Extreme Precipitation Under Historical and Future Global Warming. Stanford University

Wang Y, Cao Z, Au S-K (2011) Practical reliability analysis of slope stability by advanced Monte Carlo simulations in a spreadsheet. Can Geotech J 48:162–172. https://doi.org/10.1139/T10-044

Wong FS (1985) First-order, second-moment methods. Comput Struct 20:779–791

Yang Z, Ching J (2019) A novel simplified geotechnical reliability analysis method. Appl Math Model 74:337–349. https://doi.org/https://doi.org/10.1016/j.apm.2019.04.055

Zhang R, Goh ATC, Li Y, et al (2021) Assessment of apparent earth pressure for braced excavations in anisotropic clay. Acta Geotech 16:1615–1626. https://doi.org/10.1007/s11440-020-01129-x

Zhang RH, Goh ATC, Zhang WG (2019) System reliability assessment on deep braced excavation adjacent to an existing upper slope in mountainous terrain: a case study. SN Appl Sci 1:876. https://doi.org/10.1007/s42452-019-0938-x

Zhang T, Baroth J, Dias D, Nejjar K (2024) Deterministic and probabilistic analysis of great-depth braced excavations: A 32 m excavation case study in Paris. J Rock Mech Geotech Eng 16:1505–1521.

https://doi.org/https://doi.org/10.1016/j.jrmge.2023.12.006

Zhang W, Liu H (2022) Probabilistic Analysis on Excavation Responses BT - Design of Deep Braced Excavation and Earth Retaining Systems Under Complex Built Environment: Theories and Case Studies. In: Zhang W, Liu H (eds). Springer Singapore, Singapore, pp 201–210

Zhao J, Ritter S, DeJong MJ (2022) Early-stage assessment of structural damage caused by braced excavations: Uncertainty quantification and a probabilistic analysis approach. Tunn Undergr Sp Technol 125:104499. https://doi.org/https://doi.org/10.1016/j.tust.2022.104499